UDC 536.2
DOI: 10.37128/2520-6168-2024-1-1

APPLICATION OF THERMAL ANEMOMETRY FOR TURBULENT FLOW ASSESSMENT

Grygorii KALETNIK, Academician of NAAS of Ukraine, Doctor of Economic Sciences, Professor
Vitalii YANOVYCH, Doctor of Technical Sciences, Professor
Svitlana LUTKOVSKA, Doctor of Economics Sciences, Professor
Yurii POLIEVODA, Candidate of Technical Sciences, Associate Professor
Olena SOLONA, Candidate of Technical Sciences, Associate Professor
Vinnytsia National Agrarian University

КАЛЕТНІК Григорій Миколайович, академік НААН України, д.е.н., професор
ЯНОВИЧ Віталій Петрович, д.т.н, професор
ЛУТКОВСЬКА Світлана Михайлівна, д.е.н., професор
ПОЛЄВОДА Юрій Алікович, к.т.н., доцент
СОЛОНА Олена Василівна, к.т.н., доцент
Вінницький національний аграрний університет

This paper is devoted to a review of the physical principle and effective methodology of thermal anemometry. Its uniqueness lies in the ability to realize a comprehensive high-frequency assessment of the dynamic and thermal state of the turbulent flow. It is worth noting that the American Nobel Prize winner in physics Richard Feynman called turbulence "the most important unsolved problem of classical physics", since there is no direct description of this phenomenon according to classical principles. Therefore, its physical interpretation is still considered one of the six most important mathematical issues of our time. Thus, despite its long history, thermal anemometry remains one of the leading techniques for studying of turbulent flow. Which has a significant impact on hydromechanical and heat-mass exchange processes, particularly in food technology.

One of the most common types of thermal anemometry is the Hot-Wire anemometer, where a thin platinum wire is used as a sensor. The principle of operation of the anemometer is to maintain a constant heating of the wire while it is cooled by the surrounding flow of liquid or gas. Thus, the power required to compensate for the thermal state of the sensor wire correlates with the flow rate.

The first part of the paper is devoted to the description of the physical principles of thermal anemometry, its advantages and limitations. In particular, special attention is paid to the mathematical interpretation of the heat transfer process between the incremental element of the sensor wire and the surrounding flow. After that, the paper provides a detailed analysis of the design features and practical application of various types of wire sensors. Finally, the last section discusses the calibration methodology and various approaches to the linearization procedure of the obtained calibration curves. Among them, the linearization method based on the Collis-Williams law deserves special attention, since it provides highly accurate interpolation of calibration data and takes into account the temperature compensation of the sensor.

Key words: *thermal anemometry, heat transfer, turbulent flow, sensor types, calibration, linearization approaches*

Eq. 34. Fig. 4. Ref. 30.

1. Problem formulation

A Hot-Wire Anemometer or thermal anemometer is a fundamental tool for accurately measuring instantaneous flow velocity. This method has found numerous applications in a wide variety of industries and is used by large companies, research institutions, and universities around the world [1-9].

The main principle of the HWA revolves around the consideration of the thermal state of the sensor, which is influenced by the convective heat transfer occurring between the wire and the surrounding flow. There are three primary modes of probe operation: Constant-Current Mode (CCA), Constant-Temperature Mode (CTA), and Constant Voltage Anemometer Mode (CVA) [10-13]. The distinction lies in how they regulate the temperature of the sensor wire. In CCA and CVA modes, the thermal anemometer maintains a constant current and voltage respectively, to ensure a consistent heat flow from the wire to the fluid. In contrast, the CTA mode is designed to maintain a stable wire temperature [14]. Thus, while CCA and CVA models are well-suited for

accurate measurement of temperature and its fluctuations, CTA mode is better for measuring flow velocity and conducting detailed assessments of turbulence.

2. Analysis of recent research and publications

Despite its long history, the hot-wire anemometer remains one of the primary research tools in fluid dynamics, particularly for turbulent flow studies. Hot-wire anemometry offers unique advantages in fluid measurement, making it an essential tool for aeronautics, fluid dynamics research, and education.

One of the most significant benefits of hot-wire anemometry is its ability to accurately measure flow velocities with a high-frequency resolution, reaching up to several hundred kilohertz [1, 15]. Furthermore, the physical principle of hot-wire anemometry allows for the simultaneous evaluation of both the velocity and thermal fluctuations of the perturbed flow.

While hot-wire anemometry has many advantages, it also has some disadvantages and limitations. A notable disadvantage is related to the delicate nature of its probe. The thin wire element is susceptible to damage from excessive bending, vibration, or exposure to contaminants in the fluid. Such damage can result in inaccurate readings or even complete failure of the hot-wire sensor. Additionally, unlike Particle Image Velocimetry (PIV), hot-wire anemometry cannot measure the velocity field simultaneously. It can only measure the velocity at a single point at any given moment. Consequently, to acquire a comprehensive understanding of the velocity field, a supplementary traverse system must be employed to move the probe through the flow. The limitations of this method are often associated with its significant sensitivity to temperature fluctuations. As an example, a slight temperature shift of 1° C can result in an error of approximately 2% in the obtained results. Therefore, determining the velocity near a solid wall, where the process of convection heat transfer between the flow and the wall occurs, presents notable challenges. According to Finn [15], the critical distance, typically ranging from 0.1 to 0.2 mm, varies depending on the ambient velocity. Nonetheless, hot-wire anemometry remains a valuable tool for researchers studying fluid dynamics. Each researcher must consider the advantages, disadvantages, and limitations of hot-wire anemometry to make informed decisions about when and how to use the technique to obtain accurate and meaningful results.

As previously discussed, the fundamental principle of a thermomagnetometry relies on the heat transfer occurring between the sensitive element (wire) of the probe and the ambient flow. Consequently, the dimensions of the wire and the environment surrounding the probe are considered to assess the heat transfer characteristics [16]. The probe's construction typically involves bulky prongs and a delicate wire, as depicted in Fig. 1. This design facilitates the localization of heat exchange towards the prongs and concentrates the temperature distribution within the wire. The thermal state of the probe can be analysed by expressing the heat-rate balance of a wire segment dx.

$$\dot{Q}_e = d\dot{Q}_{fc} + d\dot{Q}_c + d\dot{Q}_r + d\dot{Q}_s. \quad (1)$$

The Hot-Wire involves one part of a Wheatstone bridge, where the wire resistance is kept constant over the bandwidth of the feedback loop.

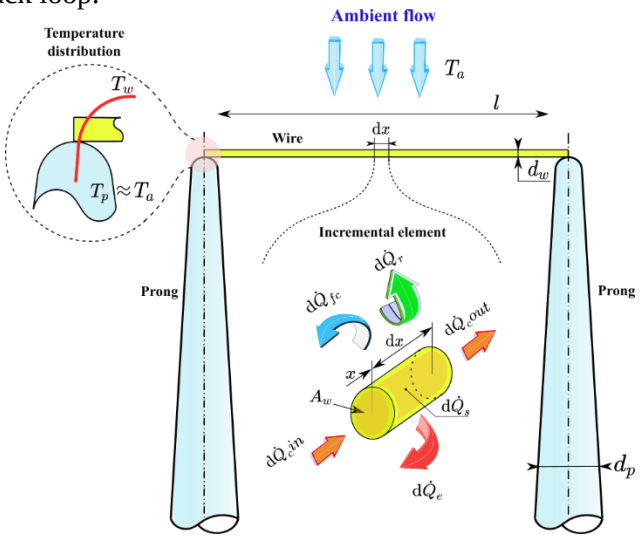

Fig. 1. Principal interpretation of the heat transfer process between the probe and ambient flow

From a physical point of view, the left part of eq.2 reflects "Joule's first law" [17], which describes the heat-generation rate $d\dot{Q}_e$ by a current flow through a wire.

$$d\dot{Q}_e = \frac{I^2 \chi_w}{A_w} dx, \quad (2)$$

where χ_w is the electrical resistivity of the wire material with cross-section A_w at characteristic temperature T_w. While the right side of the eq. 1 interprets the dissipation of the generated thermal energy in the surround due to a combination of forced-convection $d\dot{Q_{fc}}$, conduction $d\dot{Q}_c$, radiation $d\dot{Q}_r$, and heat storage rate $d\dot{Q}_s$. Logically, most of the released wire heat is dissipated to the environment by convection. According to Newton's law of cooling, the forced-convective heat-transfer rate $d\dot{Q_{fc}}$ is directly proportional to the temperature difference between the wire T_w and the ambient T_a flow. Moreover, the analytical interpretation of Newton's law, thanks to the coefficient of convective heat transfer h, establishes a connection between the heat flow and the properties of the liquid flow.

Principle interpretation of the heat transfer process between the probe and ambient flow:

$$d\dot{Q_{fc}} = \pi d_w h(T_w - T_a)dx, \quad (3)$$

where d_w is the diameter of the wire.

The value of the conductive heat-transfer rate $d\dot{Q}_c$ can be estimated using Fourier's law [18]. According to it, the amount of heat passing through an elementary isothermal surface is proportional to the temperature gradient and the area through which the heat spreads. Basically, the appearance of the gradient is associated with the holder, the relatively large size of which leads to the dissipation of thermal energy transmitted from the heated wire.

$$d\dot{Q}_c = -k_w A_w \frac{\partial^2 T_w}{\partial x^2} dx, \quad (4)$$

where k_w is the thermal conductivity of the wire material at temperature T_w.

The radiative heat-transfer rate $d\dot{Q}_r$ from the wire to the surround can be determined as:

$$d\dot{Q}_r = \pi d_w \sigma \xi (T_w^4 - T_a^4)dx, \quad (5)$$

where σ is the Stefan-Boltzmann constant and ξ is the emissivity of the sensor.

Typically, the value of $d\dot{Q}_r$ is small and usually ignored when evaluating the overall thermal condition of a hot wire sensor. Finally, last but not least, the heat storage rate can be described as:

$$d\dot{Q}_s = \rho_w c_w A_w \frac{\partial T_w}{\partial t} dx, \quad (6)$$

where ρ_w and c_w is the density and specific heat capacity of the wire, respectively.

Based on the above dependencies, the general heat-rate balance eq.1 can be represented in the following form.

$$\frac{I^2 \chi_w}{A_w} - \pi d_w h(T_w - T_a) + k_w A_w \frac{\partial^2 T_w}{\partial x^2} - \rho_w c_w A_w \frac{\partial T_w}{\partial t} = 0. \quad (7)$$

It should be noted that the material properties and geometry of the wire strongly affect the overall dynamics of heat transfer processes. For example, the increase in wire length l_w is accompanied by linear growth of forced-convective heat-transfer activities. While the reduction of the wire heat-transfer area $A_w = 4/\pi d_w^2$ and the application of the wire material with a low thermal conductivity coefficient k_w greatly minimize the effect of conductive end losses. Therefore, the active length of the wire is usually much greater than the diameter $l_w \gg d_w$. In general, the heat-transfer realized between the wire segment and the surrounding can be interpreted as the equivalent of electrical power $P = \frac{I^2 \chi_w}{A_w} = I^2 R_w$, which is necessary to maintain a constantly heated state of the wire. Thus, assuming that heat storage and radiant heat-transfer rate are insignificant, and the conductive heat-transfer to the two prongs is negligible, the heat balance relationship for a wire segment can be written as follows:

$$I^2 R_w = \pi l_w d_w h(T_w - T_a) = \pi k l_w (T_w - T_a) Nu, \quad (8)$$

where R_w is the actual resistance of the wire, while $T_w - T_a$ is the temperature difference between the heated sensor and the ambient flow, k is the thermal conductivity of the fluid and Nu is the Nusselt number.

As mentioned earlier, due to the conductive activity of the prongs, the temperature T_w and resistance R_w along the heated wire do not have a constant value. Thus, an integration operation is usually used to estimate their average characteristics:

$$T_w = \frac{1}{l_w} \int_{l_w} T_w dx, \quad (9)$$

and

$$R_w = \int_{l_w} \frac{\chi_w}{A_w} dx, \quad (10)$$

where χ_w is resistivity of wire material with cross-sectional area A_w and dx represents the increment in the length of the wire.

According to [19, 20], the relationship between material resistance and temperature variation has a linear character and can be expressed as:

$$R_w = R_a[1 + \alpha_a(T_w - T_a)], \quad (11)$$

where R_a and α_a represent the resistance and temperature coefficient at reference temperature, respectively, characterizing the cold state of the probe.

Furthermore, a simple mathematical rearrangement of eq.11 enables the establishment of the connection between the cold and warm states of the wire. This ratio is called as the overheating ratio a.

$$(T_w - T_a)\alpha_a = a = \frac{R_w - R_a}{R_a}. \quad (12)$$

Based on the pioneering experimental and theoretical work of King, the convective heat transfer is frequently represented by the following expression:

$$Nu = A + BRe^n, \quad (13)$$

where A, B and n are empirical constants, while Re is Reynolds number.

It is interesting to mention that King based his derivations on the assumption of potential flow, which is a poor approximation to real flow around a wire at low Reynolds numbers, so King's derivation is in some sense flawed.

It should be noted that King's conclusions assume of potential flow, which is an inaccurate approximation for natural flow around a wire at low Reynolds numbers. As a result, King's derivation can be considered flawed to some extent [21]. Nevertheless, this law has been the considered tool for fitting calibration data in practical hot-wire anemometry for almost a hundred years [22]. Substituting eq. 13 into eq. 7 yields the following dependency:

$$I^2R_w = \pi k_w l_w (T_w - T_a)\left[A + B\left(\frac{\rho d_w}{\mu}\right)U^n\right], \quad (14)$$

where U is velocity of the ambient flow, ρ is the density and μ is the kinematic viscosity of the ambient flow.

As per King's law, the coefficient *n* is usually a square root. However, in practical terms, *n* is determined through the calibration procedure to compensate for conductive end losses. Bruun [2, 16, 23] reported that these losses may contribute up to 15% of the overall heat transfer of the wire.

Usually, the eq. 14 is used in the simplified form.

$$I^2R_w = A + BU^n(T_w - T_a), \quad (15)$$

where l_w, k_w, d_w, π, ρ, and μ included in the constant coefficients A and B at the calibration process.

Finally, using Ohm's law $E_w = IR_w$, the thermal state of the heated wire is easily interpreted in voltage.

$$\frac{E_w^2}{R_w} = A + BU^n(T_w - T_a). \quad (16)$$

The above equation clearly indicates that the hot-wire voltage is sensitive to both velocity and the temperature of the air.

The most common class of probes is a hot-wire probe. The thin wire is typically made of platinum, tungsten, or nickel-chromium alloy and is suspended between two prongs. Usually, wire probes have a 5 μm diameter and their ends are copper- and gold-plated to a thickness of 15 to 20 μm, leaving an active sensor of 1.25 mm in the middle of the wire. Depending on the number of installed sensors, probes can be presented in a single, double, or triple configuration (see Fig. 2 a, b). Each sensor incorporated in a probe enables the extension of dimensional space for flow estimation. Moreover, the design of the prongs can have a different shape, depending on the probe's intended purpose. For example, to measure the boundary layer, the prongs can be placed below the axis of the probe or even bent perpendicular to it. Thus, that design allows realized measurements near a solid wall without flow disturbance from the probe body.

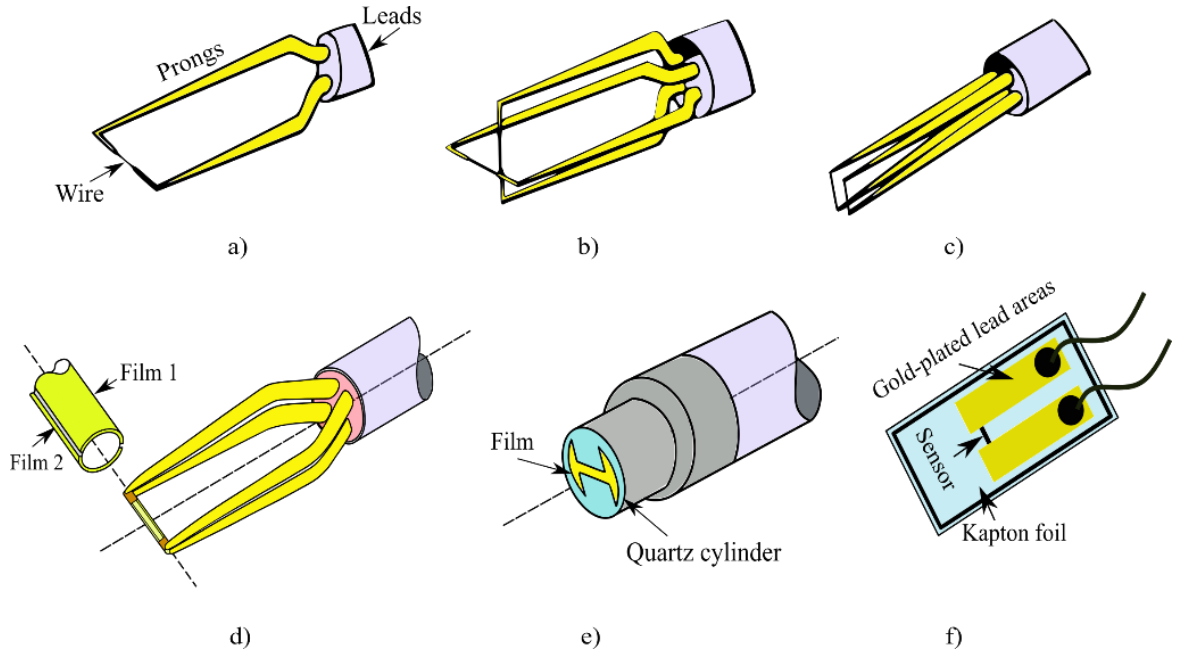

Fig. 2. Some types of probes: a) Single gold-plated wire probe; b) Dual-sensor gold-plated wire probes; c) Parallel array wire probe; d) Split-fiber probes; e) Flush-mounting film probes; f) Glue-on probe

It should mention that the number of sensors does not always correspond to the number of flow measurement directions. There are also combination probes that use multiple sensors and can offer unique capabilities. For example, there is a special probe with two parallel straight prongs to assess the extremely low level of turbulence (see Fig. c). Thus, two sensors placed close to each other allow simultaneous measurement of the same flow fluctuation in one dimension [24, 25]. Another interesting example of a combined probe is the temperature-compensated miniature wire probe. In this case, the wire functions as a velocity sensor, while the coil operates as a temperature sensor. This type is particularly useful in determining the flow velocity at rapid temperature fluctuates [26].

Due to the delicacy of hot-wire probes, as alternative, hot-film probes have been developed. They consist of metal-film parts deposited on a quartz or polymer substrate to provide electrical isolation. The exposed surfaces of the sensor are additionally covered with quartz or varnish to prevent contamination and abrasion. The high breakdown voltage of quartz enables the probe to operate across a wide range of temperatures, and its thermal coefficient of expansion is compatible with commonly used nickel covering, thus avoiding signal distortion [27]. Generally, hot-film probes can be categorized as cylindrical and non-cylindrical sensors. The first group comprises fiber-film probes, while the second group primarily represents flush-mounting film probes in different configurations.

Typically, fiber-film probes are cylindrical sensors made of 70 μm diameter, 3 mm long quartz fibers with a nickel-thin film layer about 0.1 μm thick. While the copper- and gold-plated fiber ends are soldered to the probe pins, leaving a sensitive length of 1.25 mm. These probes are more durable than wire probes and less susceptible to contamination, making them an excellent choice for use in harsh environments such as gas or liquid applications. Constructively fiber-film probes can be represented by single, dual, or triple sensors, allowing one, two, or three flow components evaluation, respectively. Moreover, there are also split fiber probes, which contain only a single quartz fiber coated with two parallel nickel films (see Fig. 2 d). Thus, they can replace dual-sensor fiber probes (X-probes) for estimating two flow components.

As mentioned earlier, a feature of the flush-mounting probe is the absence of a cylindrical core. Instead, the active sensing element is represented as a line or ring of thin nickel foil deposited on surfaces of different shapes. For example, widespread the sensor placed on the flat end of a quartz cylinder (see Fig. 2 e). In this case, the probes are installed through a hole in the wall, with the flat plane of the cylinder positioned precisely at the same level as the wall. Another variant of the flush-mounting probe that should be mentioned is the glue-on or adhesive probe [28] (see Fig. 2 f). Where the sensor is placed on thin Kapton foil and sticks directly on the wall at points of interest. Generally, the primary function of the non-cylindrical sensors is to measure skin friction (wall shear stress) in boundary layers [29].

3. The purpose of the article

The primary objective of this paper is to consolidate the theoretical frameworks and offer practical guidelines for the efficient application of the Hot-Wire anemometry.

4. Results of the researches

The calibration is typically conducted using a specialized calibrator featuring a low-turbulence-free jet, where the velocity is determined based on the pressure drop at the exit. Alternatively, calibrations can also be performed within the wind tunnel itself, using a pitot tube as the reference for velocity determinations.

Typically, the first step in calibration involves estimating the electrical resistance of the probe. For practical hot wire applications, room temperature is often chosen as the reference temperature. Therefore, the manufacturer usually provides information about the value of resistance R_{20} and temperature coefficient α_{20} at 20 ℃ (cold state). However, in order to assess the probe's performance, it is common practice to independently calculate its specific resistance in the cold state. Thus, the following formula can be applied:

$$R_{20} = \frac{R_a}{1+(T_a-20)a_{20}}, \quad (17)$$

where R_a probe resistance at ambient temperature T_a.

The value of R_a can be easily determined through direct measurements of the total resistance of the probe and its supplementary components R_{tot}.

$$R_a = R_{tot} - (R_C + R_S + R_L), \quad (18)$$

where R_C, R_S, and $R_L$represent the resistances of the connection cable, support, and leads of the probe, respectively.

To determine the distinct values of the first two parameters, specific shorting probes are employed. While the value of R_L is usually specified by the manufacturer. It should be noted that as the value of the reference temperature is changed so will the corresponding value of α_a with:

$$\alpha_a = \left(R_0 \cdot {R_a}^{-1}\right)\alpha_0, \quad (19)$$

where R_0 and α_0 resistance and temperature coefficient at 0 ℃.

Thus, generally, to calculate the hot state of the wire, the eq. 11 can be rewritten as follows:

$$R_w = R_{20}[1 + \alpha_{20}(T_w - T_{20})], \quad (20)$$

where T_w is operational temperature of the heated wire, typically at 200 ℃.

In general, the calibration procedure is provided for establishing a relationship between the anemometer output signal and the corresponding velocity of the ambient flow. To achieve this, the probe is exposed to a range of known velocities U, and the corresponding voltages E are recorded. Subsequently, by performing a curve fitting procedure on the data points E and U, a transfer function is derived, enabling the conversion of voltage measurements into precise velocity values. Sometimes, this procedure is also called linearization. Traditionally, a 4-order polynomial (eq. 21) and power function (eq. 22) are commonly employed for the curve fitting process [18].

$$U = C_0 + C_1E + C_2E^2 + C_3E^3 + C_4E^4, \quad (21)$$

where C_0 to C_n are the calibration constants.

Polynomial fitting is a frequently used method for linearization due to its accuracy. However, it is important to emphasize that the resulting equation should be strictly limited to the range of velocities used during calibration. Deviating from this range can lead to significant distortions in the linearization curve, ultimately affecting the accuracy of the velocity calculations. Additionally, it is worth mentioning that the polynomial method utilizes a traditional linear scale during the calibration process. In contrast, when employing the power method or King's law [29] for fitting, it becomes imperative to work with a double logarithmic scale.

$$E^2 = A + B \cdot U^n, \quad (22)$$

where A, B and n are the calibration constants. Typically, n is 0.4-0.45.

Meanwhile, it is essential to consider that the power fitting method demonstrates lower accuracy in comparison to polynomial fits, particularly when dealing with wide velocity ranges. This discrepancy can be attributed to the sensitivity of the exponent n in the power law equation to variations in velocity. This is the reason why it is usually recommended to be used within a moderate velocity range of $U_{min}/U_{max} \approx 10 - 20$.

Thus, by applying the determination calibration coefficients and the voltage from the sensor, the equivalent velocity value can be easily obtained by the following relation.

$$U = \left(\frac{E^2}{B} - A\right)^{1/n}. \quad (23)$$

In addition to the methods mentioned earlier, the "extended power law" has also gained popularity due to its ability to work in a wide range of rates $0.01 < Re < 500 \cdot 10^3$.

$$E^2 = A + BU^n + CU, \tag{24}$$

where U can be obtained by a simple inversion process and C is an individual constant for each probe.

Nonetheless, a key drawback of the above techniques is the need for output signal correction in cases where the ambient temperature deviates from the temperature used during the calibration process.

$$E_{corr} = \left(\frac{T_w - T_r}{T_w - T_a}\right) E_a, \tag{25}$$

where E_a represents the acquired voltage, and T_r, T_a, and T_p denote the reference temperature, ambient temperature, and probe's hot state temperature, respectively. This expression is applicable for moderate temperature fluctuations, within a range of $\approx \pm 5$℃ [2].

To avoid this drawback, linearization based on the Collis-Williams law has become widespread (eq.26). Where the left part is responsible for heat transfer, while the right one is the relationship of the King's law [29]. The key advantage of this method is the ability to provide more accurate linearization of temperature-dependent sensor by compensating for their nonlinear behavior.

$$Nc = Nu \left(\frac{T_m}{T_a}\right)^M = A + B \cdot Re_w^N, \tag{26}$$

where T_m, Nu and Re_w are mean temperature, Nusselt number and wire thickness-based Reynolds number, respectively. While A, B, N, M are calibration coefficients.

$$Nu = \frac{R_w E^2}{\pi l_w \lambda_w (T_w - T_a)(20 + R_w + R_l + R_p)}, \tag{27}$$

where $\lambda_w = 0.183 \cdot 10^{-3} T_m^{0.87}$ is thermal conductivity of air.

$$T_m = 0.5(T_a + T_w), \tag{28}$$

where T_a and T_w are ambient and heated wire temperature.

Thus, in order to implement this linearization process, it is first necessary to plot a curve for Re_w and N_c based on the collected experimental data. Subsequently, aligning the acquired values with King's law enables the determination of the values A, B, N, and M.These coefficients provide straightforward calculation of the Reynolds numbers depending on the Nusselt numbers obtained from the hot-wire signal.

$$Re_w = \left(\frac{N_c - A}{B}\right)^{\frac{1}{N}}. \tag{29}$$

Finally, the flow velocity can be easily determined as follows:

$$U = \frac{Re_w \nu_m}{d_w}, \tag{30}$$

where $\nu_m = 73.51 \cdot 10^{-6} \frac{T_m^{1.75}}{P_{bar}}$ is kinematic viscosity of air and P_{bar} is barometric pressure.

As an example, Fig. 3 shows the calibration curves for a parallel array 55P71 hot wire probe where the calibration process is implemented simultaneously for two sensors. It should be mentioned, that the overall uncertainty related to the conversion of the electric signal from the hot wire into a velocity measurement sample is approximately $\pm 0.5\%$.

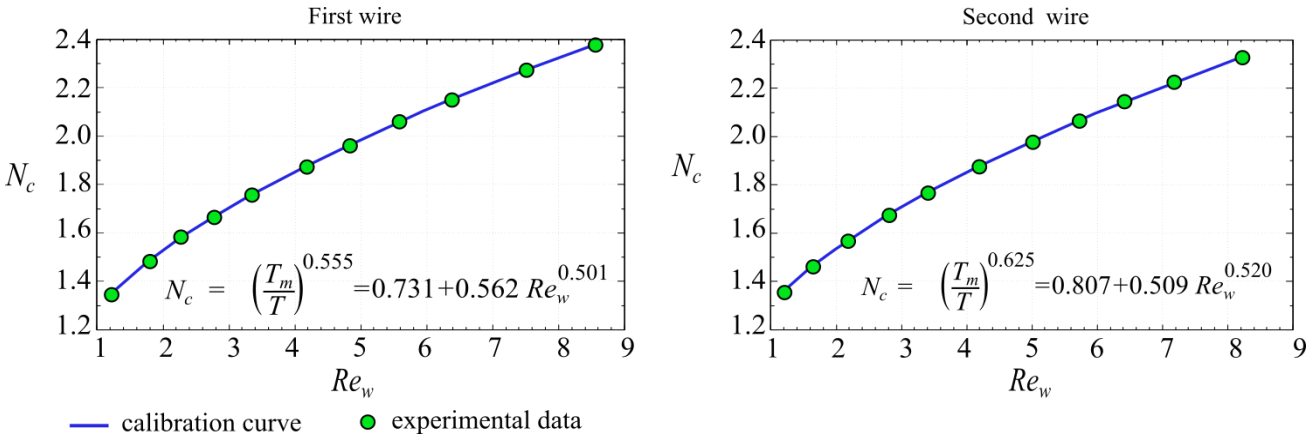

Fig. 3. Calibration curves for the parallel array 55P71 hot-wire probe

Unlike unidirectional probes, which measure only one flow component, the calibration of multi-sensor probes should also include the evaluation of individual directional sensitivity coefficients. Consequently, for

dual-axial probe, the yaw factor k is applied to represent the sensitivity of each sensor to the flow direction. Whereas in the case of tri-axial probe, the directional sensitivity is described by both the yaw k and the pitch h coefficients.

Thus, the calibration procedure of the X-wire probe 55P64, which contains two perpendicular wires, can be presented as follows (see Fig. 4). First, each probe sensor is calibrated separately when its orientation directly coincides with the flow direction ($\alpha = 0°$). Subsequently, with a constant input flow velocity, the magnitudes of streamwise U and spanwise V velocities are computed depending on the probe rotation angle α relative to the flow direction. Its typically carried out within a range of $\pm 45°$, with the axis passing through the crossing point of the wires perpendicular to the wire plane. Afterward, the calculated flow velocity at each angle is compared to the maximum velocity within the entire range of angles [$U(\alpha)/U_{max}$and $V(\alpha)/V_{max}$], which is usually observed at $\alpha = 0°$. Fig. 4 illustrates the influence of the probe's rotation angle, known as the "yaw effect," on the flow velocity calculation. In most cases, fitting the obtained curves can be implemented by following function:

$$\frac{U(\alpha)}{U_{max}} = \left[\left\langle cos\left((\alpha + 45°)\cdot \pi/180°\right)\right\rangle^2 + k_u^2\left\langle sin\left((\alpha + 45°)\cdot \pi/180°\right)\right\rangle^2\right]^{1/2}, \quad (31)$$

and

$$\frac{V(\alpha)}{V_{max}} = \left[\left\langle cos\left((\alpha + 45°)\cdot \pi/180°\right)\right\rangle^2 + k_v^2\left\langle sin\left((\alpha + 45°)\cdot \pi/180°\right)\right\rangle^2\right]^{1/2}, \quad (32)$$

where k_u^2 and k_v^2 represent the squared yaw factors for the streamwise and spanwise directions, respectively.

Thus, the determination of the “yaw coefficients” is simplified to the curve fitting process, which can be easily realized in Excel by the Solver function. It should be noted that the yaw coefficients for X-array probes are typically nearly equal, and their values, which vary depending on the type of probe, can be found in the Dantek recommendations [15]. Finally, after determining the values of k_u^2 and k_v^2, the velocity components in the streamwise U and spanwise V directions can be calculated by classical relations:

$$U = \frac{\sqrt{2}}{2}[(1 + k_v^2)\cdot V^2 - k_v^2 \cdot U^2]^{1/2}, \quad (33)$$

and

$$V = \frac{\sqrt{2}}{2}[(1 + k_u^2)\cdot U^2 - k_u^2 \cdot U^2]^{1/2}. \quad (34)$$

The general calibration principle of X-wire probe 55P64 is shown in Fig.4.

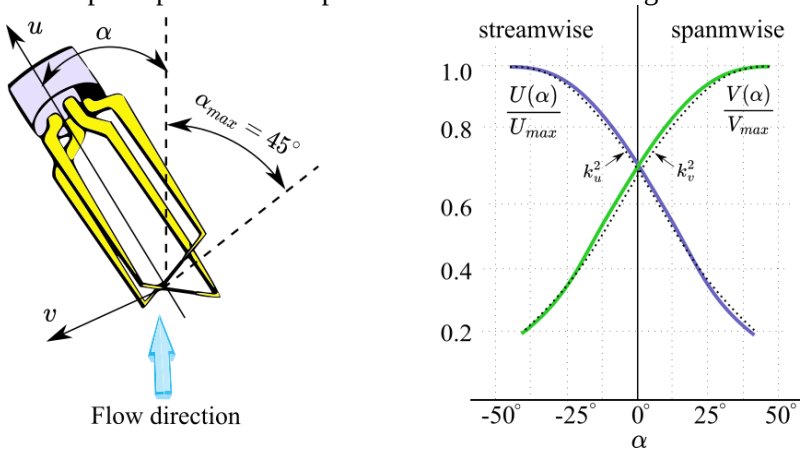

Fig. 4. Principle of the direction calibration X-wire 55P64 probe

5. Conclusions

Nowadays, many researchers and manufacturers are increasingly focused on developing new and improving existing methods to accurately assess flow conditions. One of the fundamental methods is thermal anemometry. The significance of this method cannot be overstated, as it provides an accurate measurement of instantaneous flow velocity with high-frequency resolution. Therefore, the obtained data allow us to estimate not only the average velocity values but also to determine the structure of turbulence.

One of the most common types of thermal anemometry is Constant Temperature Anemometry or simply Hot-Wire. Its basic principle involves maintaining the hot wire at a constant thermal state using the Wheatstone Bridge to measure changes in wire resistance with temperature. When the wire cools, the system

supplies extra energy to maintain a stable temperature, and the power required corresponds to the cooling rate and the flow velocity passing the sensor.

Overall, this paper provides an in-depth analysis of practical experience, advantages, limitations, and practical recommendations for the effective application of Hot-Wire anemometry. Among them, the linearization method based on the Collis-Williams law deserves special attention. Since, it provides high-precision interpolation of calibration data and also takes into account sensor temperature compensation.

References

[1] Bruun, H. (1996). Hot-Wire Anemometry: Principles and Signal Analysis. *Measurement Science and Technology*, *7 (10).* DOI: 10.1088/0957-0233/7/10/024. [in English].

[2] Bruun, H. (2001). Interpretation of a hot wire signal using a universal calibration law. *Journal of Physics E: Scientific Instruments*, *4 (3),* 225. DOI: 10.1088/0022-3735/4/3/016. [in English].

[3] Yanovych, V., Duda, D., Uruba, V. (2020). Structure turbulent flow behind a square cylinder with an angle of incidence. 2021. *European Journal of Mechanics, B/Fluids, 85,* 110–123. DOI: 10.1016/j.euromechflu.2020.09.003. [in English].

[4] Yanovych, V., Duda, D., Uruba, V. Antoš, P. (2021). Anisotropy of turbulent flow behind an asymmetric airfoil. *SN Applied Sciences, 3 (12),* 1–16. DOI: 10.1007/s42452-021-04872-2. [in English].

[5] Yanovych, V., Duda, D., Uruba, V., Tomášková, T. (2022). Hot-Wire Investigation of Turbulence Topology behind Blades at Different Shape Qualities. *Processes, 10 (3),* 2–22. DOI: 10.3390/pr10030522. [in English].

[6] Yanovych, V., Duda, D., Uruba, V., Procházka, P., Antoš, P. (2022). Effect of Cylinder Roughness on Strouhal Number. *In Proceedings Topical Problems of Fluid Mechanics 2022*, 201–207 DOI: 10.14311/TPFM.2022.027. [in English].

[7] Yanovych, V., Duda, D., Uruba, V. Antoš, P. (2022). Drag Estimation in the Near Wake of the NREL's Airfoils Based on Hot-Wire Data. *The Application of Experimental and Numerical Methods in Fluid Mechanics and Energy*, *369,* 02012. DOI: 10.1051/matecconf/202236902012. [in English].

[8] Yanovych, V., Duda, D., Uruba, V., Kosiak, P., Horáček, V. (2022). Turbulence topology behind different sections of the wind turbine blade. *Conference on Power System Engineering*, *367,* 00023. DOI: 10.1051/matecconf/202236700023. [in English].

[9] Gatski, Th., Bonnet, J.P. (2009). *Compressibility, Turbulence and High Speed Flow.* DOI: 10.1016/B978-0-08-044565-6.X0001-2. [in English].

[10] Sivakami, V., Pal, A., Balasubramanian, V. (2020). Realization of constant voltage anemometer using an alternative signal conditioning circuit. *Experimental Techniques*, *44 (4),* 1–11. DOI: 10.1007/s40799-020-00379-4. [in English].

[11] Sarma, G.R. (1993). Analysis of a constant voltage anemometer circuit. *Instrumentation and Measurement Technology Conference*. Irvine, CA, USA. Publisher IEEE. 731–736. DOI: 10.1109/IMTC.1993.382547. [in English].

[12] Kegerise, M., Spina, E. (2020). A comparative study of constant-voltage and constant-temperature hot-wire anemometers Part I: The static response. *Experiments in Fluids*, *29,* 154–164. DOI: 10.1007/s003489900073. [in English].

[13] Bestion, D., Gaviglio, J., Bonnet, J.P. (1983). Comparison between constantcurrent and constant-temperature hot-wire anemometers in high-speed flows. *Review of Scientific Instruments*, *54 (11),* 1513–1524. DOI: 10.1063/1.1137279. [in English].

[14] Jørgensen, F. (2001). *How to measure turbulence with hot-wire anemometers - a practical guide.* Dantec Dynamics, Denmark. [in English].

[15] Bruun, H. (1975). On the temperature dependence of constant temperature hotwire probes with small wire aspect ratio. *Journal of Physics E: Scientific Instruments*, *8 (11),* 942. DOI:10.1088/0022-3735/8/11/018. [in English].

[16] Besson, U. (2012). The history of the cooling law: When the search for simplicity can be an obstacle. *Science and Education*, *21,* 1085–1110. DOI: 10.1007/s11191-010-9324-1. [in English].

[17] Lienhard, J.H., Lienhard, J.H. (2024). *A Heat Transfer Textbook.* 6th Edition. Cambridge MA: Phlogiston Press, https://ahtt.mit.edu. [in English].

[18] Laufer, J., Mcclellan, R. (1956). Measurements of heat transfer from fine wires in supersonic flows. *Journal of Fluid Mechanics*, *1 (3),* 276–289. DOI: 10.1017/S0022112056000160. [in English].

[19] Hinze, J. (1959). *Turbulence: An Introduction to its mechanism and theory.* 1st Edition. McGraw-Hill, USA. [in English].
[20] Kazi, S.N. (2012). An Overview of Heat Transfer Phenomena. DOI: 10.5772/2623. [in English].
[21] Lundstrom, H., Sandberg, M., Moshfegh, B. (2007). Temperature dependence of convective heat transfer from fine wires in air: A comprehensive experimental investigation with application to temperature compensation in hot-wire anemometry. *Experimental Thermal and Fluid Science, 32(2),* 649–657. DOI: 10.1016/j.expthermflusci.2007.08.002. [in English].
[22] Bruun, H. (1979). Interpretation of hot-wire probe signals in subsonic airflows. *Journal of Physics E: Scientific Instruments, 12 (12),* 1116. DOI: 10.1088/0022-3735/12/12/001. [in English].
[23] Sekiya, N., Matsumoto, A. (2009). Development of a hot-wire probe with two parallel wires placed closely together. *Journal of Fluid Science and Technology, 4 (1),* 95–106. DOI: 10.1299/jfst.4.95. [in English].
[24] Antos, P., Uruba, V. (2012). Hot-wire measurement in turbulent flow behind a parallel-line heat source. *Proc. Appl. Math. Mech., 12,* 493–494. DOI: 10.1002/pamm.201210235. [in English].
[25] Khamshah, N., Abdalla, A., Koh, S., Rashag, H. (2011). Issues and temperature compensation techniques for hot wire thermal flow sensor: A review. *International Journal of Physical Sciences, 6 (14),* 3270–3278. DOI: 10.5897/IJPS11.630. [in English].
[26] Atkins, M.A., Barratt, M.D. (2016). *Application of Thermo-Fluidic Measurement Techniques.* 1st Edition. [in English].
[27] Rendon, C., Ruan, Zh., Ruiz, O. (2020). Skin-friction measurements in turbulent boundary layers. *International Journal of Engineering and Technology, 12 (1),* 1–15. DOI: 10.21817/ijet/2020/v12i1/201201002. [in English].
[28] Genevieve, C.B. (2003). Hot-wire anemometry. *Annual Review of Fluid Mechanics, 8 (1),* 209–231. DOI: 10.1146/annurev.fl.08.010176.001233. [in English].
[29] King, L.V., Barnes, H.T. (1914). On the convection of heat from small cylinders in a stream of fluid: Determination of the connection constants of small platinum wires with applications to hot-wire anemometry. *Philosophical Transactions of the Royal Society of London. Series A, 90,* 563–570. DOI: 10.1098/rspa.1914.0089. [in English].

ЗАСТОСУВАННЯ ТЕПЛОВОЇ АНЕМОМЕТРІЇ ДЛЯ ОЦІНКИ ТУРУБЛЕНТНОГО ПОТОКУ

Дана стаття присвячена огляду фізичного принципу та ефективній методології застосування теплової анемометрії. Унікальність якої полягає в здатності реалізувати комплексну високочастотну оцінку динамічного та теплового стану турбулентного потоку. Варто відзначити, що Американський лауреат Нобелівської премії з фізики Річард Фейнман назвав турбулентність "найважливішою невирішеною проблемою класичної фізики", оскільки не існує прямого опису даного явища згідно класичних принципів. Тому його фізична інтерпретація досі вважається одним з шести найважливіших мате математичних питань сьогодення. Таким чином незважаючи на свою довгу історію, теплова анемометрія залишається однією з провідних методик для дослідження закономірностей розвитку турбулентного потоку, який має суттєвий вплив на інтенсифікацію гідромеханічних та тепломасообмінних процесів різноманітних харчових технологій.

Одним з найпоширеніших видів теплової анемометрії є анемометр з гарячим дротом, де у якості сенсора використовується тонкий платиновий дріт. Принцип дії анемометра полягає в підтримці постійного нагріву дроту, в той час як він охолоджується навколишнім потоком рідини або газу. Таким чином, потужність, необхідна для компенсації теплового стану сенсорного дроту, корелює зі швидкістю потоку.

Перша частина статті присвячена опису фізичних принципів роботи теплової анемометрії її переваг та недоліків. Зокрема, особливу увагу приділено математичній інтерпретації процесу теплопередачі між інкрементним елементом сенсорного дроту та навколишнім потоком. Після чого, у роботі проводиться детальний аналіз конструктивних особливостей та практичне застосування різних типів дротяних сенсорів. Нарешті, в останньому розділі розглянуто методологію калібрування та різні підходи до процедури лінеаризації отриманих калібрувальних кривих. Серед яких особливу увагу заслуговує метод лінеаризації на основі закону Колліса-Вільямса, оскільки він забезпечує високоточну інтерполяцію калібрувальних даних та враховує температурну компенсацію сенсора.

Ключові слова: *теплова анемометрія, тепловіддача, турбулентний потік, типи сенсорів, калібрація, лінеаризаційні підходи*

Ф. 34. Рис. 4. Літ. 29.

INFORMATION ABOUT THE AUTHORS

Grygorii KALETNIK – Academician of the NAAS of Ukraine, Doctor of Economics, Professor, Head of the Department of Administrative Management and Alternative Energy Sources of Vinnitsa National Agrarian University (Soniachna Str., 3, Vinnitsa, Ukraine, 21008, e-mail: rector@vsau.org, https://orcid.org/0000-0002-4848-2796).

Vitalii YANOVYCH – Doctor of Technical Sciences, Professor of the Department of Labor Protection and Biotechnical Systems in Animal Husbandry of Vinnytsia National Agrarian University (St. Soniachna, 3, Vinnytsia, Ukraine, 21008, e-mail: yanovichvitaliy@gmail.com, https://orcid.org/ 0000-0002-8152-7124).

Svitlana LUTKOVSKA – Doctor of Economics Sciences, Professor, Vice-rector for scientific, pedagogical and educational work Vinnytsia National Agrarian University (21008, Vinnytsia, 3 Soniachna st, e-mail: svetvsau@gmail.com, https://orcid.org/0000-0002-8350-5519).

Yurii POLIEVODA – Candidate of Technical Sciences, Associate Professor of the Department of Technological Processes and Equipment of Processing and Food Industries of Vinnytsia National Agrarian University (St. Soniachna, 3, Vinnytsia, Ukraine, 21008, e-mail: vinyura36@gmail.com, https://orcid.org/0000-0002-2485- 0611).

Olena SOLONA – Candidate of Technical Sciences, Associate Professor of the Department of Labor Protection and Biotechnical Systems in Animal Production of Vinnytsia National Agrarian University (St. Soniachna, 3, Vinnytsia, Ukraine, 21008, e-mail: solona_o_v@ukr.net, https://orcid.org/ 0000-0002-4596-0449).

КАЛЕТНІК Григорій Миколайович – академік НААН України, доктор економічних наук, професор, завідувач кафедри адміністративного менеджменту та альтернативних джерел енергії Вінницького національного аграрного університету (вул. Сонячна, 3, м. Вінниця, Україна, 21008, e-mail: rector@vsau.org, https://orcid.org/0000-0002-4848-2796).

ЯНОВИЧ Віталій Петрович – доктор технічних наук, професор кафедри охорони праці та біотехнічних систем у тваринництві Вінницького національного аграрного університету (вул. Сонячна, 3, м. Вінниця, Україна, 21008, e-mail: yanovichvitaliy@gmail.com, https://orcid.org/0000-0002-2485-0611).

ЛУТКОВСЬКА Світлана Михайлівна – доктор економічних наук, професор, проректор з науково-педагогічної та навчальної роботи Вінницького національного аграрного університету (вул. Сонячна, 3, м. Вінниця, 21008, e-mail: svetvsau@gmail.com, https://orcid.org/0000-0002-8350-5519).

ПОЛЄВОДА Юрій Алікович – кандидат технічних наук, доцент кафедри технологічних процесів та обладнання переробних і харчових виробництв Вінницького національного аграрного університету (вул. Сонячна, 3, м. Вінниця, Україна, 21008, e-mail: vinyura36@gmail.com, https://orcid.org/0000-0002-8152-7124).

СОЛОНА Олена Василівна – кандидат технічних наук, доцент кафедри охорони праці та біотехнічних систем у тваринництві Вінницького національного аграрного університету (вул. Сонячна, 3, м. Вінниця, Україна, 21008, e-mail: solona_o_v@ukr.net, https://orcid.org/0000-0002-4596-0449).